Mon. Not. R. Astron. Soc. **000**, 1–?? (2015) Printed September 24, 2015 (MN LaTeX style file v2.2)

arXiv:1509.06911v1 [astro-ph.CO] 23 Sep 2015

Do radio mini-halos and gas heating in cool-core clusters have a common origin?

L. Bravi[1,2], M. Gitti[1,2], G. Brunetti[2]∗
[1] *Physics and Astronomy Department, University of Bologna, via Ranzani 1, 40127 Bologna, Italy*
[2] *INAF, Osservatorio di Radioastronomia, via Gobetti 101, I-40129 Bologna, Italy*

ABSTRACT

In this letter we present a study of the central regions of cool-core clusters hosting radio mini-halos, which are diffuse synchrotron sources extended on cluster-scales surrounding the radio-loud brightest cluster galaxy. We aim to investigate the interplay between the thermal and non-thermal components in the intra-cluster medium in order to get more insights into these radio sources, whose nature is still unclear. It has recently been proposed that turbulence plays a role for heating the gas in cool cores. By assuming that mini-halos are powered by the same turbulence, we expect that the integrated radio luminosity of mini-halos, νP_ν, depends on the cooling flow power, $P_{\rm CF}$, which in turn constrains the energy available for the non-thermal components and emission in the cool-core region. We carried out a homogeneous re-analysis of X-ray *Chandra* data of the largest sample of cool-core clusters hosting radio mini-halos currently available (~ 20 objects), finding a quasi-linear correlation, $\nu P_\nu \propto P_{\rm CF}^{0.8}$. We show that the scenario of a common origin of radio mini-halos and gas heating in cool-core clusters is energetically viable, provided that mini-halos trace regions where the magnetic field strength is $B \gg 0.5\,\mu$G .

Key words: Galaxies: clusters – Radio continuum: mini-halos – galaxies: jets – galaxies: cooling flows

1 INTRODUCTION

The amount of gas in cool-core clusters that is cooling radiatively to low temperatures is found to be much less than what is predicted by the standard cooling flow model (e.g., Fabian 1994; Peterson & Fabian 2006, for reviews). The implication is that the central intra-cluster medium (ICM) of these "cool-core clusters" must experience some kind of heating to balance cooling. The most promising source of heating has been identified as feedback from energy injection by the active galactic nucleus (AGN) of the brightest cluster galaxy (BCG) (e.g., McNamara & Nulsen 2007, 2012; Gitti et al. 2012; Fabian 2012, and reference therein). At the same time, mechanically-powerful AGN are likely to drive turbulence in the central ICM which may contribute to gas heating. In this context, Zhuravleva et al. (2014) recently found that the AGN-driven turbulence must eventually dissipate into heat and it is sufficient to offset radiative cooling. On the other hand, such turbulence can also play a role for particle acceleration and magnetic field amplification in the ICM.

Diffuse synchrotron emission has been observed in a number of cool-core clusters in the form of "radio mini-halos" surrounding the radio-loud BCG (e.g., Feretti et al. 2012; Brunetti & Jones 2014, for reviews). Mini-halos, which have steep ($\alpha \sim 1.1$, $S(\nu) \propto \nu^{-\alpha}$) radio spectra and amorphous (roundish) shape, extend on scales $\sim 100-500$ kpc (total size) tracing regions where the ICM cooling time is short and the ICM is compressed. The origin of mini-halos is still unclear and it has generated a lively discussion in the last decade (e.g., Brunetti & Jones 2014). One possibility is that they form through the re-acceleration of relativistic particles by turbulence (Gitti et al. 2002, 2004; Mazzotta & Giacintucci 2008; ZuHone et al. 2013). Alternatively they may be of hadronic origin (Pfrommer & Enßlin 2004; Zandanel et al. 2014).

In this letter we assume a re-acceleration scenario where the turbulence is responsible for both the origin of mini-halos and for quenching cooling flows. In the framework of this scenario, we expect a connection between the cooling flow power, $P_{\rm CF}$, and the mini-halo integrated radio power, νP_ν. A trend between νP_ν and $P_{\rm CF}$ was observed by Gitti et al. (2004, 2012) using small, heterogeneous samples of mini-halos. On the other hand, in recent years mini-halos are being found in an increasing number of cool-core clusters (e.g., Govoni et al. 2009; Giacintucci et al. 2014), thus allowing a substantial step in the field. The aim of this work

---

∗E-mail:luca.bravi@studio.unibo.it

is to overcome the limitations in the previous studies by exploiting the increased sample statistics in order to obtain more insights into the origin of mini-halos. In particular, we present the results of a homogeneous re-analysis of *Chandra* data of the largest collection of mini-halo clusters currently known ($\sim$ 20 objects, Sect. 2), and investigate the connection between the thermal properties of cool cores and the non-thermal properties of mini-halos (Sect. 3). We further discuss the consistency of the adopted turbulent model and derive constraints on the magnetic field in the mini-halo region (Sect. 4). We adopt a ΛCDM cosmology with $H_0 = 70$ km s^{-1}Mpc^{-1}, $\Omega_M = 1 - \Omega_\Lambda = 0.3$.

2 MINI-HALO SAMPLE AND X-RAY DATA

2.1 Sample selection

Our sample is obtained from the list of 21 mini-halos reported in Giacintucci et al. (2014), who recently selected a large collection of X-ray-luminous clusters from the *Chandra* ACCEPT[1] sample (Cavagnolo et al. 2009) with available high-quality radio data from archival VLA (Very Large Array) and GMRT (Giant Metrewave Radio Telescope) observations, and discovered four new mini-halos. We further included the new mini-halo detection in the Phoenix cluster (van Weeren et al. 2014).

X-ray *Chandra* archival observations are available for all clusters. To ensure a uniform quality to the X-ray data, we excluded shallow observations, with an exposure time $<$ 20 ks. Furthermore, we have considered only the observations where the cluster core emission, which corresponds to the location of the cooling region and of the mini-halo we are interested in, is well pointed and enclosed in the central chip. This guarantees that the data reduction process is performed in a homogeneous, consistent manner for all the objects in our sample. The full mini-halo sample used in this work finally comprises 20 objects, listed in Table 1, where we report the radio properties taken from the literature (Giacintucci et al. 2014; van Weeren et al. 2014). By excluding the objects classified by Giacintucci et al. (2014) as "candidate" or "uncertain", we further selected a subsample of 16 confirmed mini-halos.

2.2 Chandra data preparation

Data were reprocessed with CIAO 4.6, using CALDB 4.5.9 and corrected for know time-dependent gain problems following techniques similar to those described in the *Chandra* analysis threads[2]. Screening of the event files was applied to filter out strong background flares. Blank-sky background files, filtered in the same manner as in each cluster and normalized to the count rate of the source image in the 9.0-12.0 keV band, were used for background subtraction. We identified and removed the point sources in the CCD using the CIAO task `WAVEDETECT`. Images, instrument maps, and exposure maps were created in the 0.5 - 7.0 keV band. Data with energies above 7.0 keV and below 0.5 keV were excluded in order to prevent background contamination and uncertainties in the ACIS calibration, respectively.

3 SPECTRAL ANALYSIS AND RESULTS

3.1 Cool-Core spectral analysis

In order to extract the azimuthally averaged profiles of the physical parameters of the thermal ICM, we created concentric annuli centred on the peak of the X-ray emission of each cluster. For each annulus was extracted a single spectrum that was then modelled using the XSPEC code, version 12.8.1g. Spectral fitting was performed in the [0.5 - 7] keV band. In order to correct the projection effects we fitted the spectra using a `projct*wabs*apec` model. The free parameters in this model are temperature kT, metallicity Z (measured relative to the solar values) and normalization parameters of the `apec` model. The hydrogen column density was fixed at the Galactic value (Dickey & Lockman 1990). The deprojected fits allow us to derive a radial profile of the temperature, kT, and of the electron density, $n_{\rm e}$. With this two quantities, we estimated the cooling time as the time necessary for the ICM to radiate its enthalpy per unit volume:

$$t_{\rm cool} = \frac{5}{2}\frac{kT}{\mu X_H n_e \Lambda(T)} \qquad (1)$$

where $\mu = 0.61$ is the molecular weight for a fully ionized plasma, $X_H = 0.71$ is the hydrogen mass function, and $\Lambda(T)$ is the cooling function (we have interpolated the table by Sutherland & Dopita (1993) as a function of temperature and metallicity Z). The cooling radius $r_{\rm cool}$ is traditionally defined as the radius at which $t_{\rm cool}$ is equal to the age of the systems, usually taken to be the look-back-time at $z = 1$, $t_{\rm cool} \sim 7.7$ Gyr. However, in this work we adopted a shorter time interval in which the system has realistically been relaxed, i.e. the time since the last merger event, $t_{\rm cool} = 3$ Gyr. Accounting for the different definitions of $t_{\rm cool}$, our estimates, reported in Table 1, are in agreement with the cooling radii of the ACCEPT sample (Cavagnolo et al. 2009). We note that the radius of the mini-halo, $R_{\rm MH}$, is generally larger than our definition of $r_{\rm cool}$, corresponding in cooling times in the range 4 Gyr $\div$ $t_{\rm Hubble}$. This readly implies that the region of strong cooling is smaller than the mini-halo extension.

3.2 Spectral analysis in the mini-halo region

In order to determine the physical properties of the thermal ICM in the region where the diffuse radio emission is present, we extracted a single spectrum inside $R_{\rm MH}$ for each cluster of the sample. The spectra are modelled using a `wabs*(apec+mkcflow)` model[3]. The model assumes a combination of a standard single temperature emission (`apec` component) and of a multi-phase component that takes into account a isobaric cooling flow emission, `mkcflow` (Arnaud 1996). This model fit provides a direct estimate of the amount of gas that is cooling. Under the assumptions that the thermal component represents the ambient cluster atmosphere and that the cooling flow component is cooled ambient gas, the higher temperature and metallicity parameters of the `mkcflow` component were tied to those of the

---

[1] Archive of Chandra Cluster Entropy Profiles Tables.

[2] http://cxc.harvard.edu/ciao/threads/index.html.

[3] We also used a `projct*wabs*(apec+mkcflow)` model that corrects for the contribution of the foreground emission projected along the line-of-sight. The results are consistent within the errors with those of the projected model `wabs*(apec+mkcflow)`.

Table 1. Properties of our sample of mini-halo clusters.

Cluster name	z	$S_{\mathrm{MH}\,[1.4\mathrm{GHz}]}$ (mJy)	r_{cool} (kpc)	R_{MH} (kpc)	$\nu P_{\nu\,[1.4\mathrm{GHz}]}$ 10^{40} erg s^{-1}	kT (keV)	$\dot{M}$ ($M_{\odot} yr^{-1}$)	P_{CF} 10^{44} erg s^{-1}	Notes
2A 0335+096	0.035	21.1 ± 2.1	46 ± 1	70	0.08 ± 0.01	$2.85^{+0.02}_{-0.03}$	$111.9^{+4.8}_{-4.7}$	0.32 ± 0.02	
A 2626	0.055	18.0 ± 1.8	17 ± 2	30	0.19 ± 0.01	$2.95^{+0.24}_{-0.23}$	$4.3^{+1.8}_{-1.7}$	0.02 ± 0.01	U
A 1795	0.063	85.0 ± 4.9	39 ± 2	100	1.11 ± 0.07	$4.62^{+0.08}_{-0.04}$	$21.1^{+6.7}_{-8.8}$	0.10 ± 0.04	C
ZwCl 1742.1+3306	0.076	13.8 ± 0.8	32 ± 1	40	0.28 ± 0.01	$3.04^{+0.11}_{-0.10}$	$30.1^{+5.7}_{-5.4}$	0.09 ± 0.02	U
A 2029	0.077	19.5 ± 2.5	35 ± 1	270	0.39 ± 0.06	$7.58^{+0.11}_{-0.11}$	$9.6^{+8.9}_{-6.0}$	0.07 ± 0.05	
A 478	0.088	16.6 ± 3.0	45 ± 1	160	0.45 ± 0.08	$6.01^{+0.14}_{-0.14}$	$20.8^{+36.8}_{-20.8}$	< 0.34	
A 2204	0.152	8.6 ± 0.9	50 ± 1	50	0.76 ± 0.07	$4.21^{+0.08}_{-0.08}$	< 0.01	< 0.06	
RX J1720.1+2638	0.159	72.0 ± 4.4	46 ± 2	140	7.46 ± 0.45	$5.05^{+0.18}_{-0.17}$	$0.02^{+38.80}_{-0.01}$	< 0.20	
RXC J1504.1-0248	0.215	20.0 ± 1.0	64 ± 1	140	3.78 ± 0.20	$5.87^{+0.35}_{-0.30}$	$606.2^{+419.5}_{-396.0}$	3.5 ± 2.4	
A 2390	0.228	28.3 ± 4.3	38 ± 1	250	6.24 ± 0.94	$8.01^{+0.39}_{-0.36}$	$69.0^{+98.5}_{-68.0}$	< 1.34	
A 1835	0.252	6.1 ± 1.3	57 ± 1	240	1.66 ± 0.35	$7.64^{+0.35}_{-0.14}$	$295.2^{+154.5}_{-81.3}$	2.25 ± 0.90	
MS 1455.0+2232	0.258	8.5 ± 1.1	55 ± 1	120	2.45 ± 0.32	$4.61^{+0.26}_{-0.23}$	$242.4^{+206.1}_{-187.5}$	1.11 ± 0.91	
ZwCl 3146	0.290	~ 5.2	60 ± 1	90	1.95 ± 0.01	$5.73^{+0.37}_{-0.29}$	$276.7^{+165.4}_{-149.3}$	1.58 ± 0.90	
RX J1532.9+3021	0.345	7.5 ± 0.4	67 ± 1	100	4.69 ± 0.24	$5.28^{+0.57}_{-0.30}$	$647.8^{+411.8}_{-331.1}$	3.41 ± 1.98	
MACS J1931.8-2634	0.352	47.9 ± 2.8	61 ± 1	100	28.0 ± 1.7	$6.11^{+1.01}_{-0.60}$	$1178.0^{+524.9}_{-511.0}$	7.17 ± 3.30	U
RBS 797	0.354	5.2 ± 0.6	69 ± 1	120	3.08 ± 0.34	$5.46^{+0.42}_{-0.28}$	$59.2^{+491.9}_{-59.1}$	< 3.00	
MACS J0159.8-0849	0.405	2.4 ± 0.2	53 ± 1	90	1.95 ± 0.20	$6.59^{+3.32}_{-0.79}$	$106.7^{+484.3}_{-106.7}$	< 3.90	C
MACS J0329.6-0211	0.450	3.8 ± 0.4	54 ± 1	70	3.98 ± 0.42	$4.83^{+1.13}_{-0.52}$	$126.6^{+569.3}_{-126.6}$	< 3.36	C
RX J1347.5-1145	0.451	34.1 ± 2.3	62 ± 2	320	35.8 ± 2.5	$21.6^{+14.3}_{-4.6}$	$2852.3^{+399.1}_{-473.7}$	61.3 ± 29.1	
Phoenix	0.596	6.8 ± 2.0	73 ± 1	176	14.1 ± 4.2	$10.8^{+14.5}_{-2.6}$	$4353.2^{+3744.0}_{-4353.0}$	< 121.81	

Notes: Col. (1): Cluster name. Col. (2): Redshift. Col. (3): Mini-halo flux density at 1.4 GHz from Giacintucci et al. (2014), except in the case of Phoenix where the value was estimated from the observations at 610 MHz (van Weeren et al. 2014) by assuming a spectral index of $\alpha = 1.1$. Col. (4): Cooling radius corresponding to a cooling time of 3 Gyr. Col. (5): Average radius of the mini-halo estimated by Giacintucci et al. (2014) as $R_{\mathrm{MH}} = \sqrt{R_{\mathrm{max}} \cdot R_{\mathrm{min}}}$, where R_{max} and R_{min} are the maximum and minimum radius as derived from the $+3\sigma$ isocontour of the image. For consistency, we have used this equation to estimate R_{MH} of the Phoenix cluster from the published maps of van Weeren et al. (2014). Col. (6): Radio power of mini-halos at 1.4 GHz (in terms of integrated radio luminosity, νP_{ν}). Col. (7): Temperature of the `apec` component of the `wabs*(apec+mkcflow)` spectral model inside R_{MH}. Col. (8): Mass accretion rate derived from the normalization parameter of the `mkcflow` component inside R_{MH}. Col. (9): Cooling flow power estimated as $P_{\mathrm{CF}} = \frac{\dot{M}kT}{\mu m_p}$ inside R_{MH}. Col. (10): Uncertain (U) and candidate (C) mini-halos according to Giacintucci et al. (2014).

`apec` component. Contrary to the previous spectral analysis in concentric annuli, here the hydrogen column density was not fixed to the Galactic value since a different best-fit value was often preferred by the fit. Furthermore, according to the physics of a standard cooling flow model, the lower temperature was fixed to the lowest possible value (∼ 0.1 keV). The (free) normalization parameter of the `mkcflow` model is the mass deposition rate $\dot{M}$. The values of $\dot{M}$ that we obtained are in line with typical values from the literature and with independent estimates derived for some of our clusters by different authors (e.g., Rafferty et al. 2006). The best-fitting parameter values and the 90% confidence level derived for each cluster are summarized in Table 1.

3.3 The correlation between νP_{ν} and P_{CF}

Gitti et al. (2004, 2012) found a correlation between the radio power of mini-halos at 1.4 GHz (in terms of integrated radio luminosity, νP_{ν}), and the cooling flow power, P_{CF}. The maximum power P_{CF} available in the cooling flow can be estimated assuming a standard cooling flow model and it corresponds to the pdV/dt work done on the gas per unit time as it enters r_{cool}:

$$P_{\mathrm{CF}} = \frac{\dot{M}kT}{\mu m_{\mathrm{p}}} \qquad (2)$$

(e.g., Fabian 1994; Gitti et al. 2004), where $\dot{M}$ is the mass deposition rate and kT is the temperature of the gas at r_{cool}. However, to compare powers emitted inside the same volume, i.e. that of the mini-halo, in this work we estimated P_{CF} inside R_{MH}. In particular, we estimated $\dot{M}$ from the normalization of the `mkcflow` component and kT from the temperature of the `apec` component[4] derived in the previous section. The values of P_{CF} are reported in Table 1.

The correlation between the radio emitted power of mini-halos at 1.4 GHz, in terms of νP_{ν}, and the cooling flow power, P_{CF}, is shown in Fig. 1. We used the bivariate correlated error and intrinsic scatter (BCES) algorithm (Akritas & Bershady 1996) to perform regression fits in log space to the data of the 12 clusters for which P_{CF} is constrained, determining the best-fitting powerlaw relationship (bisector method)[5]:

$$\log(\nu P_{\nu}) = [(0.80 \pm 0.13) \cdot \log(P_{\mathrm{CF}})] - (3.70 \pm 0.11) \qquad (3)$$

We used a Spearman test to evaluate the strength of the correlation. The Spearman parameters are r_s and *probrs*,

---

[4] The temperature kT used here is in agreement with that estimated at R_{MH} from the radial temperature profile (Sec. 3.2).

[5] We note that the upper limits on P_{CF} estimated for the other clusters are not in disagreement with the correlation.

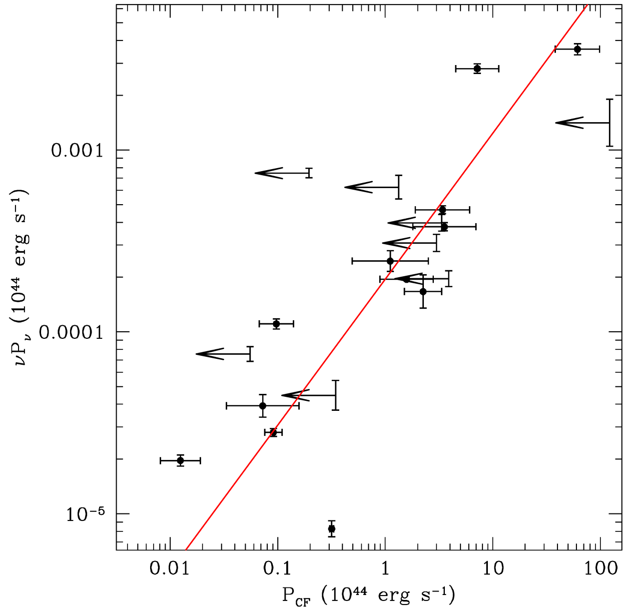

Figure 1. Correlation between the radio emitted power of mini-halos at 1.4 GHz, in terms of νP_ν, and the cooling flow power, $P_{\rm CF}$, for our sample of mini-halo clusters (see columns 6 and 9 in Table 1). The black arrows show the upper limits when $P_{\rm CF}$ is not constrained. The red line represents the best-fit relation determined without the upper limits on $P_{\rm CF}$.

where the former is a non-parametric measure of the statistical dependence between two variables and the latter is the two-sided significance level of deviation from zero. High values of r_s and small values of *probrs* indicate a significant correlation. For our data the Spearman test parameters are: $r_s = 0.89$ and $probrs = 1.14 \times 10^{-4}$, thus confirming the strength of the correlation.

The correlation is present also in the sub-sample of confirmed mini-halos[6] (Spearman test values: $r_s = 0.86$, $probrs = 6.5 \times 10^{-3}$):

$$\log(\nu P_\nu) = [(0.76 \pm 0.15) \cdot \log(P_{\rm CF,})] - (2.12 \pm 0.56) \qquad (4)$$

and it is in agreement with the best-fit relations of the full sample.

As final sanity checks, we verified that the correlation exists also if $P_{\rm CF}$ is estimated as $P_{\rm CF} = 2/5 \cdot L_{\rm cool}$ (e.g., Fabian 1994; Gitti et al. 2004), where $L_{\rm cool}$ is the cooling X–ray luminosity estimated as the total bolometric luminosity of the `wabs*(apec+mkcflow)` spectral model fitted inside $R_{\rm MH}$. Furthermore, to ensure that the trend observed in the radio luminosity - X–ray luminosity plane is not biased by any effects due to the cluster redshift, we checked that a correlation is present also in the radio flux - X–ray flux plane for the 12 clusters with well-constrained values. Finally, all correlations mentioned above are present also if $P_{\rm CF}$ is derived from the spectral analysis inside $r_{\rm cool}$.

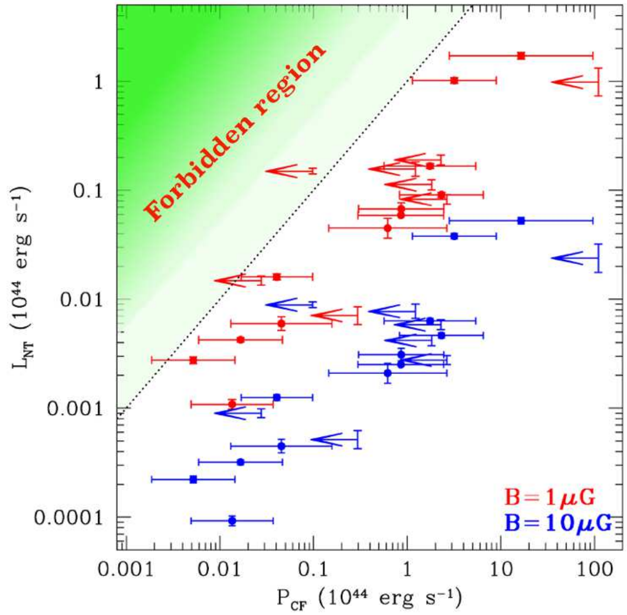

[t]

Figure 2. Correlation between $L_{\rm NT}$ and $P_{\rm CF}$ for our mini-halo cluster sample. The red and blue points were calculated assuming $B = 1\,\mu$G and $B = 10\,\mu$G, respectively. The black dotted line represents the 1:1 relation. The upper side of 1:1 relation is the forbidden region, where $L_{\rm NT} > P_{\rm H} \sim P_{\rm CF}$.

4 DISCUSSION

Starting from our mini-halo sample, having taken as robust an approach to the data as possible, we found that there are currently only a dozen clusters for which $P_{\rm CF}$ can be constrained from XSPEC spectral fitting (see Table 1). Using these clusters we have confirmed a correlation between νP_ν and $P_{\rm CF}$, revealing a connection between the energy-reservoir in cooling flows and that associated to the non-thermal components powering radio mini-halos.

A solution proposed for the cooling flow problem is based on a mechanism of heating that is distributed in the core (that is comparable to the size of radio mini-halos). This mechanism must be gentle, dissipating energy in the form of heat at a rate, $P_{\rm H}$, that cannot be much larger than the cooling power, otherwise cool cores would be disrupted. This is $P_{\rm H} \gtrsim P_{\rm CF}$. Various sources of energy capable of compensating cooling have been suggested, the most promising being heating by the feedback due to AGN (e.g., McNamara & Nulsen 2007; Fabian 2012; Gitti et al. 2012, for reviews), although details are still unclear. Recently Zhuravleva et al. (2014) analysed deep X-ray *Chandra* data of the Perseus and Virgo clusters and found that heating by turbulent dissipation evaluated in the ICM appears to balance radiative cooling locally at each radius. They suggested that turbulent dissipation may be the key mechanism responsible for compensating gas cooling losses and keeping cluster cores in an approximate steady state.

Turbulence is also proposed as an important player for the origin of mini-halos (leptonic models, Gitti et al. 2002; Mazzotta & Giacintucci 2008; ZuHone et al. 2013), although the origin of the turbulence and its connection with the thermal and dynamical properties of cool-core is still

[6] The sub-sample of confirmed mini-halos includes all clusters except those labeled with U and C in Table 1.

unclear. Here we argue that particle acceleration and gas heating in cool-cores are due to the dissipation of the same turbulence. Obviously this is a simplified picture. Indeed several turbulent components are probably generated in cool cores and may contribute in different ways to the heating of the gas and to the reacceleration of relativistic particles (see Brunetti & Jones 2014 for a review in the ICM). Anyhow, if we assume this simple picture, a fraction of $P_{\rm H}$ will be channelled into particle acceleration and non-thermal radiation. In this case, assuming $P_{\rm H} \gtrsim P_{\rm CF}$, Eq. 2 provides an upper limit to the non-thermal radiation, $L_{\rm NT}$, that can be maintained in the region of radio mini-halos for a time-scale that is longer than the radiative life-time of the relativistic electrons.

The non-thermal radiation is :

$$L_{\rm NT} = L_{\rm Syn} + L_{\rm IC} = L_{\rm Syn}\left[1 + \left(\frac{B_{\rm CMB}}{B}\right)^2\right] \qquad (5)$$

where $L_{\rm Syn}$ is the synchrotron luminosity, $L_{\rm IC}$ is the inverse Compton luminosity, $B_{\rm CMB} = 3.2\,(1{+}z)^2\,\mu$G is the magnetic field equivalent to the inverse Compton losses with CMB photons and B is the magnetic field intensity in the mini-halo region.

In Fig. 2 we report $L_{\rm NT}$ of mini-halos in our sample, estimated by assuming two reference values of $B = 1\,\mu$G and $B = 10\,\mu$G, versus $P_{\rm CF}$ measured in the hosting clusters. Magnetic fields of the order of 10 μG are estimated in cool-core clusters from current Faraday rotation studies (Carilli & Taylor 2002; Feretti et al. 2012, for reviews). In this case the scenario is found energetically consistent, namely mini-halos remain distant from the forbidden region, where $L_{\rm NT} > P_{\rm H} \sim P_{\rm CF}$. On the other hand, for weak magnetic fields, $B < 0.5\,\mu$G, we find that $L_{\rm NT} \gtrsim P_{\rm CF}$ implying that the scenario becomes not plausible. Obviously this limit can be released if we assume more complex situations where multiple turbulent components coexist in cool cores and that reacceleration of relativistic particles and gas heating are powered by different components. On the other hand, we note at the same time that relativistic particles get in general only a small fraction of the turbulent energy flux (see however Brunetti & Lazarian 2011). Consequently in the presence of weak fields, we should admit an unlikely situation where an energetic turbulent component, with specific turbulent energy $\epsilon_{\rm t} > P_{\rm CF}/M_{\rm gas}$, coexists with the gas without disturbing gas thermodynamics.

However, weak magnetic fields do not challenge only reacceleration models. Also alternative models, such as the hadronic models (e.g., Pfrommer & Enßlin 2004), are challenged in the case of $B <$ few μG, due to current gamma-ray upper limits to the π^o-decay emission obtained for nearby clusters hosting mini-halos (e.g., Aleksić et al. 2012). Consequently new theoretical scenarios will be needed if future observations provide evidence for weak magnetic fields in cool-core clusters hosting diffuse radio emission. Future observations with ASTRO-H in the hard X-rays and Faraday rotation studies with the new radio facilities, such as the JVLA and SKA precursors, are expected to contribute to constrain magnetic fields in cool-core clusters. In particular several Faraday rotation measure survey experiments are already planned such as the POSSUM survey on ASKAP (Gaensler et al. 2010), the JVLA polarization survey, VLASS (Myers 2014) and the forthcoming all-sky polarimetric survey and associated Rotation Measure grid to be carried out on SKA1_MID (Johnston-Hollitt et al. 2015).

5 SUMMARY AND CONCLUSIONS

In this work we have overcome the limitations in the previous studies by exploiting the increased statistics of known radio mini-halos that allows us to obtain further insights on their origin. In particular, we have carried out an homogeneous analysis of archival *Chandra* data of the largest existing sample of mini-halo clusters (20 objects) in order to study the X-ray properties of cool cores hosting radio mini-halos. Our main results can be summarized as follows:

- We estimated the cooling flow power, $P_{\rm CF}$, inside the mini-halo region, and compared it with the radio emitted power of mini-halos at 1.4 GHz, in terms of νP_ν. By using the 12 clusters for which the value of $P_{\rm CF}$ is constrained, we found a correlation $\nu P_\nu \propto P_{\rm CF}^{0.8}$. This suggests a connection between the thermal properties of cool-core clusters and the non-thermal properties of mini-halos, confirming the previous results obtained by Gitti et al. (2004, 2012).
- We discussed a scenario where turbulence in the cool cores is responsible for both the origin of mini-halos and for the solution of the cooling flow problem. In this context, $P_{\rm CF}$ can be regarded as an upper limit to the non-thermal luminosity $L_{\rm NT}$ generated in the mini-halo region. The limit $P_{\rm CF} \gg L_{\rm NT}$ allows us to set a corresponding lower limit $B > 0.5\,\mu$G to the typical magnetic field in mini-halos.

Future efforts and observations with ASTRO-H, JVLA, SKA-pathfinders and precursor are essential to build large mini-halo samples and achieve a full understanding of the mechanism for the origin of mini-halos (see e.g., Gitti et al. 2015, for a recent discussion about the perspectives offered by future SKA radio surveys).

ACKNOWLEDGMENTS

We thank Fabrizio Brighenti and the anonymous referee for useful comments. GB acknowledge support from von Humboldt Foundation and PRIN–INAF2014.

References

Akritas M. G., Bershady M. A., 1996, ApJ, 470, 706

Aleksić J., Alvarez E. A., Antonelli L. A., et al. 2012, A&A, 541, A99

Arnaud K. A., 1996, in Jacoby G. H., Barnes J., eds, Astronomical Data Analysis Software and Systems V Vol. 101 of Astronomical Society of the Pacific Conference Series, XSPEC: The First Ten Years. p. 17

Brunetti G., Jones T. W., 2014, International Journal of Modern Physics D, 23, 30007

Brunetti G., Lazarian A., 2011, MNRAS, 412, 817

Carilli C. L., Taylor G. B., 2002, ARA&A, 40, 319

Cavagnolo K. W., Donahue M., Voit G. M., Sun M., 2009, ApJS, 182, 12

Dickey J. M., Lockman F. J., 1990, ARA&A, 28, 215

Fabian A. C., 1994, ARA&A, 32, 277

Fabian A. C., 2012, ARA&A, 50, 455

Feretti L., Giovannini G., Govoni F., Murgia M., 2012, A&A Rev., 20, 54

Gaensler B. M., Landecker T. L., Taylor A. R., POSSUM Collaboration 2010, in American Astronomical Society Meeting Abstracts #215 Vol. 42 of Bulletin of the American Astronomical Society, Survey Science with ASKAP: Polarization Sky Survey of the Universe's Magnetism (POSSUM). p. #470.13

Giacintucci S., Markevitch M., Venturi T., et al. 2014, ApJ, 781, 9

Gitti M., Brighenti F., McNamara B. R., 2012, Advances in Astronomy, 2012, 6

Gitti M., Brunetti G., Feretti L., Setti G., 2004, A&A, 417, 1

Gitti M., Brunetti G., Setti G., 2002, A&A, 386, 456

Gitti M., Tozzi P., Brunetti G., Cassano R., et al. 2015, in Advancing Astrophysics with the Square Kilometre Array (AASKA14) The SKA view of cool-core clusters: evolution of radio mini-halos and AGN feedback. p. 76

Govoni F., Murgia M., Markevitch M., Feretti L., Giovannini G., Taylor G. B., Carretti E., 2009, A&A, 499, 371

Johnston-Hollitt M., Govoni F., Beck R., et al. 2015, Advancing Astrophysics with the Square Kilometre Array (AASKA14), p. 92

Mazzotta P., Giacintucci S., 2008, ApJ, 675, L9

McNamara B. R., Nulsen P. E. J., 2007, ARA&A, 45, 117

McNamara B. R., Nulsen P. E. J., 2012, New Journal of Physics, 14, 055023

Myers S. T., 2014, in Exascale Radio Astronomy The Karl G. Jansky VLA Sky Survey (VLASS): A Scientific and Technical Proving Ground for the SKA Era. p. 10302

Peterson J. R., Fabian A. C., 2006, Phys. Rep., 427, 1

Pfrommer C., Enßlin T. A., 2004, A&A, 413, 17

Rafferty D. A., McNamara B. R., Nulsen P. E. J., Wise M. W., 2006, ApJ, 652, 216

Sutherland R. S., Dopita M. A., 1993, ApJS, 88, 253

van Weeren R. J., Intema H. T., Lal D. V., et al. 2014, ApJ, 786, L17

Zandanel F., Pfrommer C., Prada F., 2014, MNRAS, 438, 124

Zhuravleva I., Churazov E., Schekochihin A. A., et al. 2014, Nature, 515, 85

ZuHone J. A., Markevitch M., Brunetti G., Giacintucci S., 2013, ApJ, 762, 78